CrossMark

ORIGINAL ARTICLE

MiR-142-5p promotes bone repair by maintaining osteoblast activity

Manli Tu[1] · Juanjuan Tang[4] · Hongbo He[5] · Peng Cheng[3] · Chao Chen[2]

Abstract MicroRNAs play important roles in regulating bone regeneration and remodeling. However, the pathophysiological roles of microRNAs in bone repair remain unclear. Here we identify a significant upregulation of miR-142-5p correlated with active osteoblastogenesis during the bone healing process. In vitro, miR-142-5p promoted osteoblast activity and matrix mineralization by targeting the gene encoding WW-domain-containing E3 ubiquitin protein ligase 1. We also found that the expression of miR-142-5p in the callus of aged mice was lower than that in the callus of young mice and directly correlated with the age-related delay in bone healing. Furthermore, treatment with agomir-142-5p in the fracture areas stimulated osteoblast activity which repaired the bone fractures in aged mice. Thus, our study revealed that miR-142-5p plays a crucial role in healing fractures by maintaining osteoblast activity, and provided a new molecular target therapeutic strategy for bone healing.

Keywords MicroRNA · Bone fracture · Osteoblastogenesis · *Wwp1*

✉ Peng Cheng
  cphh@sohu.com

✉ Chao Chen
  chaochen2005@163.com

1 Institute of Endocrinology and Metabolism, The Second Xiangya Hospital of Central South University, Changsha 410011, Hunan, People's Republic of China

2 Department of Endocrinology and Metabolism, The First Affiliated Hospital of Soochow University, Suzhou 215006, Jiangsu, People's Republic of China

3 Department of Gerontology, The First Hospital Affiliated to Nanjing Medical University, Nanjing 210029, Jiangsu, People's Republic of China

4 Department of Gynaecology and Obstetrics, The First Hospital Affiliated to Nanjing Medical University, Nanjing 210029, Jiangsu, People's Republic of China

5 Department of Orthopedics, Xiangya Hospital of Central South University, 87# Xiangya Road, Changsha 410008, Hunan, People's Republic of China

Introduction

Skeletal fractures, as a major social health issue, contribute to disability and morbidity especially in aged populations [1]. Approximately 1.5 million individuals experience bone fractures secondary to skeletal diseases annually [2, 3]. Nearly 5–10 % of fractures heal improperly, including delayed union or nonunion [4, 5]. The rate of bone repair is progressively reduced with aging [6]. Delayed healing results in an increased duration of immobilization and increased risk of joint stiffness. Bone healing is a complex regenerative process initiated in response to a fracture, with the final aim of restoring skeletal function. During this process, maintenance of osteoblast differentiation and activity is crucial [7]. The bone formation in fractured areas involves proliferation of osteogenic committed mesenchymal stem cells and their differentiation to mature osteoblasts, which is accompanied by synthesis of osteoid extracellular matrix proteins such as collagen type I, bone sialoprotein, osteocalcin, and osteopontin followed by matrix mineralization [8]. However, the capacity for repair declines with age; this has been determined in humans [9], rats [10, 11], and mice [12]. Aging was associated with decreased bone formation, delayed remodeling, and altered expression of genes involved in repair and remodeling [13].

MicroRNAs (miRNAs) are noncoding single-stranded, approximately 22-nucleotide RNAs that are involved in the regulation of various biological processes [14]. They play a critical role as posttranscriptional regulators of gene expression through binding to specific sequences in target genes. Recently, a growing number of novel miRNAs have been verified to control the complex process of osteogenic differentiation and osteoblastic bone formation [15–18]. Our previous studies also identified two new miRNAs (miR-2861/3960 cluster) in mouse osteoblasts that promoted osteoblast differentiation by repressing histone deacetylase 5 (*HDAC5*) and homeobox A2 (*Hoxa2*) expression at the posttranscriptional level [19, 20]. Additionally, miR-214 has been shown to target activating transcription factor 4 (*ATF4*) to inhibit osteoblast activity and bone formation both in vitro and in vivo [21]. Inhibition of miR-92a enhanced fracture healing via promotion of angiogenesis in a model of stabilized fracture in young mice [22]. However, the role of miRNAs in osteogenesis during fracture healing is still unclear.

MiR-142-5p has been shown to be overexpressed in many pathological contexts, such as gastric cancer [23], small bowel inflammation [24], simian immunodeficiency virus encephalitis [25] and atherosclerosis [26]. Remarkably, an alteration in miR-142-5p level was observed during bone development and the pathogenesis of bone diseases. The expression of miR-142-5p was downregulated in osteosarcomagenesis, as a miRNA signature defining the expression identity of osteosarcoma [27]. On the other hand, miR-142-5p expression increased during the differentiation and mineralization of osteoblasts [18, 28]. Specifically, the levels of alkaline phosphatase, Runx2, JunB, and osteocalcin increased on miR-142-5p agonist treatment, and decreased in the antagonist group. However, the role of miRNA-142-5p in bone healing remains unexplored.

In this study, we identified a significant upregulation of miR-142-5p correlated with active osteoblastogenesis during the bone healing process. We also found that the levels of miR-142-5p in the callus were lower in aged mice than in young mice and were closely associated with the age-related delay of bone healing. MiR-142-5p also promoted osteoblast activity and matrix mineralization by targeting the gene encoding WW-domain-containing E3 ubiquitin protein ligase 1 (WWP1). Thus, we postulate that a primary function of miR-142-5p in bone healing is to maintain osteoblast activity.

Materials and methods

Fracture model

All procedures involving mice were approved by the Central South University Animal Management Committee. The mice femur fracture model was constructed as previously described [29]. Mice were given an intraperitoneal injection of chloral hydrate for anesthesia. We prestabilized the right femur by placing a needle in the marrow space. A 15-mm skin incision was made along the vertical axis of the right femur, and muscles were split to expose the femur. Then, the mid-diaphysis of the femur was fractured with a nipper. Mice were euthanized at different time points, and the limbs were harvested for further analysis. All bones were assessed during surgery and during harvesting by radiography. If the fracturing procedure did not produce a stable transverse fracture or if there was evidence of the development of deep infection, the mouse was excluded from the study.

Administration of miR-142-5p in mice

Eighteen-month-old C57BL/6 mice were used in all experiments and were housed under specific pathogen–free conditions (22 °C, 12-h light/12-h dark cycles, and 50–55 % humidity) with free access to food pellets and tap water. After the femur fracture model had been constructed, these mice received once a week for 4 weeks either agomir-142-5p or negative control agomir (agomir-NC) at a dose of 2 nmol or a comparable volume of phosphate-buffered saline (PBS; 50 μl) via periosteal injection at the fracture site. Four weeks after the first injection, mice were euthanized. Bone samples were harvested for further analysis. Agomir-142-5p and agomir-NC were synthesized by Guangzhou RiboBio.

Cell culture and in vitro osteoblastic differentiation

The mouse preosteoblast cell line (MC3T3-E1) was cultured in minimum essential medium α (Gibco), supplemented with 10 % fetal bovine serum, penicillin at 100 U/ml, and streptomycin at 100 μg/ml at 37 °C with 5 % CO_2. For the experiments, confluent cells were removed with use of 0.25 % trypsin containing 10 mM EDTA, resuspended in antibiotic-free growth medium, and plated onto 24-well plates. To induce osteoblastic mineralization, MC3T3-E1 cells were seeded in 24-well plates with medium containing minimum essential medium α supplemented with ascorbic acid at 50 mg/L (Invitrogen) and 10 mM β-glycerophosphate (Sigma, St Louis, MO, USA) in a humidified 5 % CO_2 atmosphere at 37 °C. Then agomir-142-5p (200 μM) was transfected into the cells with use of Lipofectamine 2000 (Invitrogen) or antagomir-142-5p (200 μM) was directly added to the medium, and the medium was changed every 3 days. Agomir-142-5p, antagomir-142-5p, and their corresponding controls were purchased from Guangzhou RiboBio. At day 21, cells were treated with alizarin red to visualize mineralized nodules. Cells were fixed in 70 % ethanol for 1 h at room

temperature and stained with 1 % alizarin red S for 10 min. Cell preparations were washed with PBS to eliminate non-specific staining. The stained matrix was assessed with a Nikon Diaphot inverted microscope and photographed with a Nikon camera.

Quantitative reverse transcription PCR analysis

Quantitative reverse transcription PCR was done performed with a LightCycler (Roche), which is a combined thermal cycler and fluorescence detector with the ability to monitor the progress of individual PCRs optically during amplification. Total RNA from cultured cells or tissues was extracted as described previously [30]. Briefly, specimens were pooled for calluses harvested on days 0, 7, 14, 21, and 28. All specimens include 3 mm of bone, cartilage, or granulation tissue proximal and distal to the fracture site. Total RNA from harvested cells or tissues was isolated with TRIzol reagent (Invitrogen), and reverse transcription was performed with 1.0 μg total RNA and SuperScript II (Invitrogen). Amplification reactions were set up in 25-μl reaction volumes containing amplification primers and SYBR Green PCR master mix (PE Applied Biosystems). A 1-μl volume of complementary DNA was used in each amplification reaction. Preliminary experiments were conducted to optimize the primer concentrations. Primer sequences are listed in Tables S1 and S2.

Bone-specific alkaline phosphatase and osteocalcin ELISA analysis

For the bone-specific alkaline phosphatase (BALP) and osteocalcin ELISA analysis, conditioned medium was collected and stored at −80 °C until use. The BALP and osteocalcin concentration were measured with an ELISA kit according to the manufacturer's instructions (USCN Life Science).

Western blot

To investigate the expression of target proteins in cells, Western blot was performed. The protein concentrations were determined by a Bradford protein assay. For this, 100 μg protein from each sample was loaded onto a 7.5 % polyacrylamide gel. After electrophoresis, the proteins separated by sodium dodecyl sulfate–polyacrylamide gel electrophoresis were transferred to a poly(vinylidene difluoride) membrane (Millipore). The membrane was blocked with 5 % nonfat milk in PBS and then incubated with anti-WWP1, anti-Runx2, anti-JunB, anti-osteocalcin (Abcam), or anti-β-actin (Abcam) in PBS overnight. Then the membrane was reprobed with appropriate secondary antibodies conjugated with horseradish peroxidase for 1 h.

Blots were processed with an enhanced chemiluminescence kit (Santa Cruz Biotechnology), and exposed to the film.

Radiological assessment

X-ray scans of the fractured legs were serially taken at day 28 after fracture. This procedure was done with the mouse under anesthesia with the mouse supine and with both limbs fully extended. Fracture union was identified by the presence of bridging callus on two cortices. Radiographs were taken independently and blindly reviewed by three orthopedic surgeons. Radiographic images were scored as previously described [22]: grade 1, no apparent hard callus; grade 2, slight intramembranous ossification; grade 3, hard callus without bridging of the fracture gap, fracture line apparent; grade 4, hard callus with bridging of the fracture gap, fracture gap noticeable; grade 5, unclear boundary between the newly formed hard callus and existing cortical bone; and grade 6, remodeling.

The intact and fractured right femurs of each mouse were fixed with 4 % paraformaldehyde for 24 h and subsequently washed with 1X PBS. Twenty-four hours later, micro-CT scanning was performed with an eXplore Locus SP system (GE Healthcare). This machine is a cone-beam scanning system used to examine small animal specimens in vitro. Volumetric density (mg hydroxyapatite/cm^3) of the mineralized tissue of the proximal femur was measured as a fraction of the mineralized tissue within the callus, excluding the original femur shaft.

Histological assessment

Mice were euthanized on day 28 by cervical dislocation. Femurs were harvested, fixed in 10 % formalin, and embedded in paraffin. Sections were stained with hematoxylin–eosin.

Selection of potential target genes

We used TargetScan (http://www.targetscan.org/vert_50/) to predict the potential targets of miR-142-5p. We screened out 415 potential targets and searched PubMed with the keyword "osteogenesis." We selected the 11 genes mostly involved in PubMed-related articles. We ranked these 11 genes by total context score, which indicates the relevance of miR-142-5p in TargetScan (Table S3).

Wwp1 3′ untranslated region cloning and luciferase reporter assay

For functional analysis of miR-142-5p, a segment of the mouse *Wwp1* 3′ untranslated region (UTR) including the predicted miR-142-5p binding site was PCR amplified.

The PCR product was purified and then inserted into the *Xba*I–*Fse*I site immediately downstream of the stop codon in the pGL3 control luciferase reporter vector (Promega, Madison, WI, USA), resulting in wild-type pGL3–*Wwp1* 3′ UTR. A QuikChange site-directed mutagenesis kit (Stratagene, La Jolla, CA, USA) was used to introduce mutations into the seed region of mutant pGL3–*Wwp1* 3′ UTR. Then, MC3T3-E1 cells were transfected with either wild-type or mutant pGL3–*Wwp1* 3′ UTR constructs, the pRL-TK *Renilla* luciferase plasmid (Promega), and agomir-142-5p or agomir-NC for 48 h. A Dual-Luciferase reporter assay system (Promega) was used to quantify the luminescent signal with use of a luminometer (Glomax; Promega). Each value from the firefly luciferase assay was normalized to the *Renilla* luciferase value from the cotransfected phRL-null vector (Promega). The nucleotide sequences of primers for wild-type and mutant reporter plasmids are shown in Table S4.

Statistical analysis

Data are presented as the mean ± standard deviation, and all experiments were performed at least three times. Statistical analyses were performed with SPSS 16.0. Differences between the two groups were compared by the unpaired Student's *t* test, whereas more than two groups were compared by one-way analysis of variance between groups, and P values less than 0.05 were considered to be statistically significant.

Results

Identification of miR-142-5p involved in osteoblastogenesis during the bone healing process

To determine the levels of miRNAs during bone fracture healing, we screened 49 miRNAs that had previously been shown to be involved in osteogenic differentiation, bone development, and bone formation [15–18]. We identified 11 miRNAs differently expressed during the fracture healing process. The expression of miR-142-5p, miR-181a, miR-140-3p, miR-205, miR-125b, and miR-135a was upregulated. In constract, the expression of miR-130a, miR-143, miR-106a, miR-92, and miR-338 was downregulated (Fig. 1a). As the most dramatically activated miRNA, miR-142-5p was selected and we investigated its function in fracture healing. As shown in Fig. 1a, miR-142-5p was highly expressed during the whole fracture period. At 21 days after fracture, miR-142-5p expression had increased more than tenfold, and then slightly declined, coinciding with the most active part of endochondral ossification in the callus. Furthermore, the change in miR-142-5p expression was consistent with the osteocalcin messenger RNA (mRNA) level, indicating miR-142-5p might be involved in osteoblastogenesis during fracture repair (Fig. 1b).

MiR-142-5p stimulated osteoblast activity and matrix mineralization in vitro

To investigate the role of miR-142-5p in regulating osteoblast activity, we treated MC3T3-E1 cells with either agomir-142-5p (a miR-142-5p agonist) or antagomir-142-5p (a miR-142-5p inhibitor). MiR-142-5p levels in cultured cells were upregulated by agomir-142-5p transfection and markedly downregulated by antagomir-142-5p treatment (Fig. 2a). Functionally, the levels of secreted BALP and osteocalcin were markedly higher in the agomir-142-5p treatment group and lower in the antagomir-142-5p treatment group compared with the control (Fig. 2b). In addition, agomir-142-5p promoted mineralized nodule formation, whereas antagomir-142-5p treatment reduced mineralized nodule formation in 21-day cultures (Fig. 2c).

All of these results suggested that miR-142-5p stimulates osteoblast activity and matrix mineralization.

MiR-142-5p directly targeted *Wwp1*

It has been demonstrated that miRNAs execute regulatory function by binding the 3′ UTR of target gene mRNA [14]. To gain further insight into the mechanism by which miR-142-5p regulates osteoblast activity, we used TargetScan [31] to predict the potential targets of miR-142-5p. More than 400 potential targets were screened out. Among these candidate target genes, we selected 11 osteogenesis-relevant genes. *Wwp1* is one of the commonly reported genes, and is a negative regulator of osteoblast differentiation, containing a miR-142-5p binding site in the 3′ UTR [32] (Fig. 3a).

To test whether miR-142-5p can directly regulate *Wwp1*, we constructed luciferase reporters that had either a wild-type *Wwp1* 3′ UTR or a *Wwp1* 3′ UTR containing mutant sequences of the miR-142-5p binding site. We introduced luciferase reporters with agomir-142-5p into MC3T3-E1 cells and measured the level of luciferase enzyme activity to determine the effects of miR-142-5p on luciferase translation. Overexpression of miR-142-5p suppressed the luciferase activity through binding to the wild-type *Wwp1* 3′ UTR and inhibiting its expression (Fig. 3b). However, unrecognized mutant *Wwp1* 3′ UTR abolished this repression, confirming the specificity of the action (Fig. 3b).

To directly test the validity of the putative target, MC3T3-E1 cells were transfected with agomir-142-5p or antagomir-142-5p. We found no change in *Wwp1* mRNA levels for different treatment times (data not shown), but
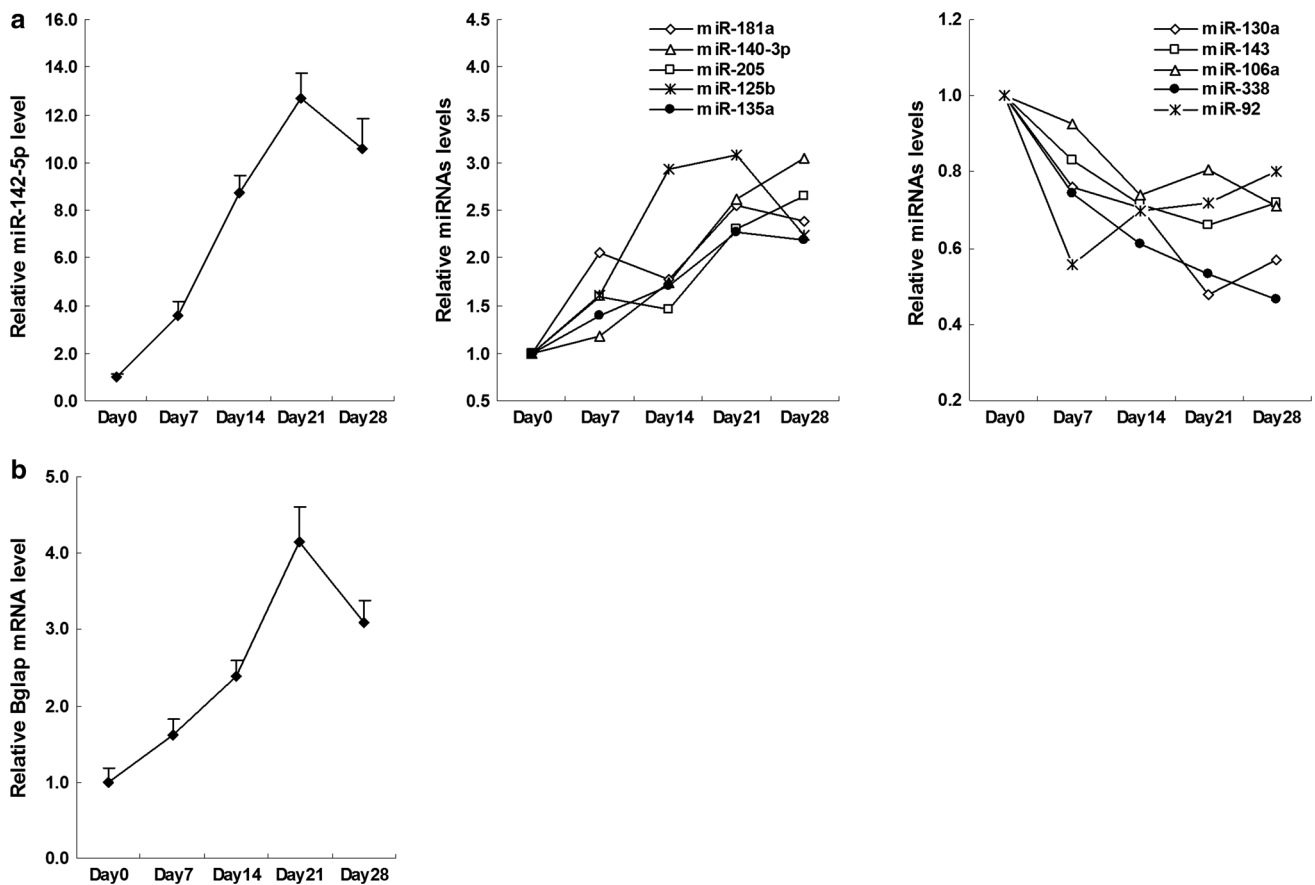
Fig. 1 miR-142-5p expression pattern during the bone healing process. **a** MicroRNA (*miRNA*) levels in callus at different time points (days 7, 14, 21, and 28 after fracture) were determined by quantitative reverse transcription PCR and normalized to the ratio of U6, then expressed as a value relative to the mean intensity at the intact femur (nonfractured; day 0); six mice per group. **b** *Bglap* (osteocalcin gene) messenger RNA (*mRNA*) levels were determined by quantitative reverse transcription PCR, and the acquired band intensities were normalized to the ratio of the internal standard β-actin and expressed as a value relative to the mean intensity at the intact femur (nonfractured; day 0); six mic per/group. Data are shown as the mean ± standard deviation

WWP1 protein levels were downregulated after agomir-142-5p treatment, whereas antagomir-142-5p treatment increased WWP1 protein expression (Fig. 3d).

Since WWP1 promotes the degradation of Runx2 and JunB in bone marrow stromal cells, we investigated Runx2 and JunB mRNA and protein levels in this process. Relative to the control, agomir-142-5p treatment induced higher levels of Runx2 and JunB mRNA and protein. In contrast, antagomir-142-5p treatment downregulated both Runx2 and JunB mRNA and protein levels (Fig. 3c, d). These results suggest that *Wwp1* is a potent target of miR-142-5p during fracture healing.

MiR-142-5p expression significantly decreased in aged mice and treatment with agomir-142-5p rescued bone formation and bone healing

It has been reported that aging is associated with a delay in fracture healing [12]. Here, we built femoral fracture repair mice models at either 10 weeks or 18 months of age. The osteocalcin and Runx2 levels decreased, whereas the WWP1 level increased in fractured areas from aged mice compared with young mice at 7, 14, 21, and 28 days after fracture, indicating impaired osteoblast activity (Fig. 4a). MiR-142-5p levels in fracture sites from young mice increased and reached a peak at 21 days after fracture (Fig. 4b). However, in aged mice, miR-142-5p levels were significantly reduced in intact bone tissue and in the entire period of the fracture repair process compared with those in young mice (Fig. 4b).

To examine whether agomir-142-5p treatment could compensate for the delayed fractures that occur in aged mice, agomir-142-5p was injected into the fracture site of 18-month-old mice once a week between day 1 and day 28 after fracture, and these mice were compared with aged mice that received agomir-NC or PBS injections.

Radiographs (Fig. 4c) showed that the callus from agomir-142-5p-treated aged mice (18-month-old mice) were calcified and mostly bridged at 28 days after fracture. The
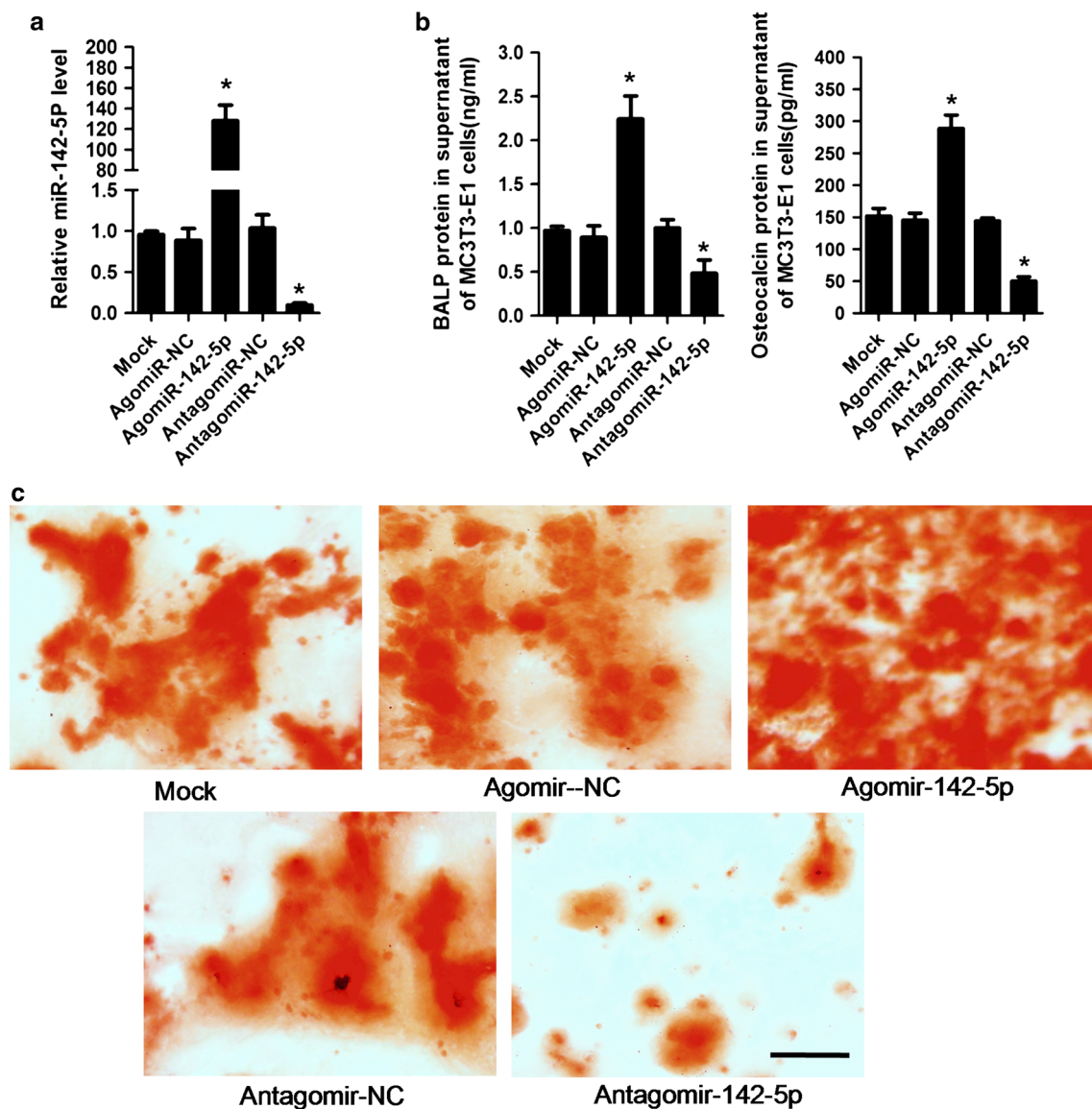
Fig. 2 MiR-142-5p stimulated osteoblast activity and matrix mineralization in vitro. **a** MC3T3-E1 cells were treated with agomir-142-5p, antagomir-142-5p, or the corresponding controls for 48 h. MiR-142-5p levels were detected by quantitative reverse transcription PCR. **b** ELISA analysis of the amount of bone-specific alkaline phosphatase (*BALP*) and osteocalcin in the supernatant of MC3T3-E1 cells after treatment with agomir-142-5p, antagomir-142-5p, or the corresponding controls for 48 h. **c** Microscopic view of the effects of miR-142-5p on matrix mineralization in MC3T3-E1 cells. Representative microscopic views at a magnification of ×200 of cells transfected with miR-142-5p, agomir-142-5p, antagomir-142-5p, or the corresponding controls after 21 days of culture are shown. All data are the mean ± standard deviation from five independent experiments. *Agomir-NC*, negative control agomir, *antagomir-NC*, negative control antagomir, *asterisk P* < 0.05, *scale bar* 500 μm

boundary between the newly formed hard callus and cortical bone became obscure. However, the callus from agomir-NC-treated aged mice and vehicle-treated aged mice was partly bridged and the gap remained. Histological analysis at 28 day after fracture showed that fractures in aged mice treated with agomir-142-5p had reduced cartilage and increased bone compared with fractures in agomir-NC-treated and vehicle-treated aged mice (Fig. 4d). Callus bone mineral density (Fig. 4e) as well as the levels of osteocalcin, Runx2, and JunB significantly increased, whereas

the WWP1 level decreased in agomir-142-5p-treated aged mice (Fig. 4f). The findings revealed that agomir-142-5p treatment resulted in improved bone formation and fracture repair in aged mice.

Discussion

Bone fracture healing is a complex regenerative process in which there are major events of bone matrix synthesis
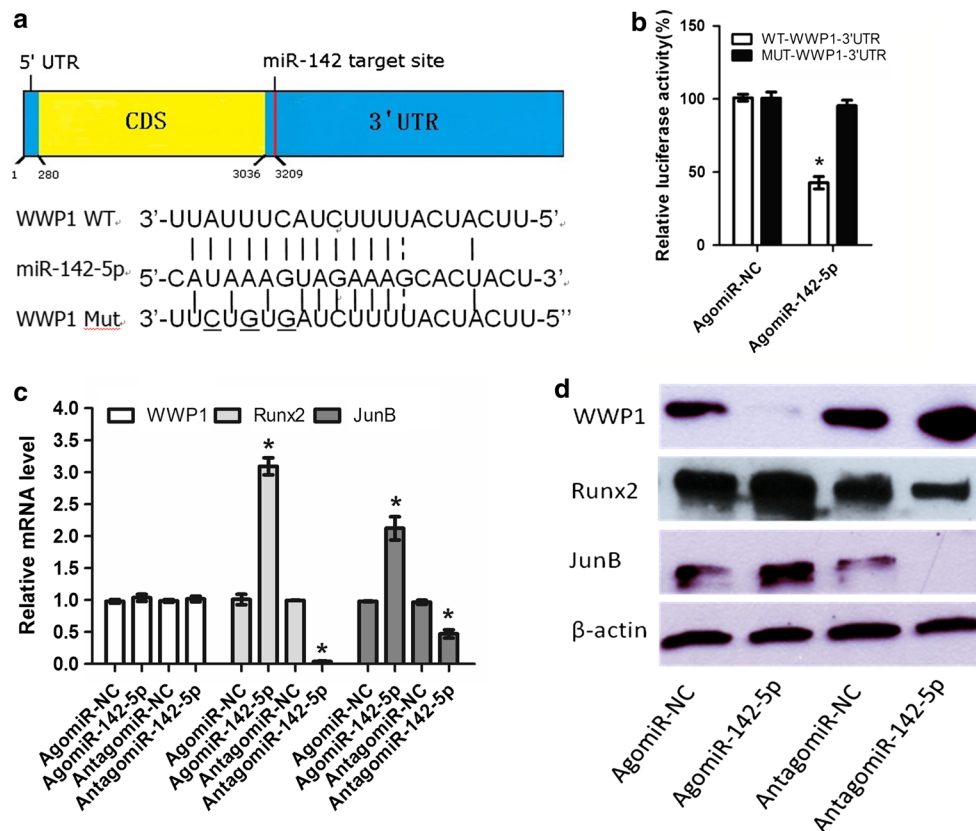
Fig. 3 MiR-142-5p directly targeted *Wwp1*. **a** The miR-142-5p putative target site in the mouse *Wwp1* 3′ untranslated region (*UTR*) and alignment of miR-142-5p with wild-type and mutant 3′ UTR regions of *Wwp1* showing the complementary pairing. The three mutated nucleotides are *underlined*. **b** The effect of agomir-142-5p, antagomir-142-5p, or the corresponding controls on luciferase activity in MC3T3-E1 cells transfected with either the wild-type *Wwp1* 3′ UTR or the mutant *Wwp1* 3′ UTR. Firefly luciferase values normalized for *Renilla* luciferase are presented. The effect of agomir-142-5p, antago-

mir-142-5p, or the corresponding controls on *Wwp1*, *Runx2*, and *Junb* messenger RNA (*mRNA*) levels (**c**) and the amount of WW-domain-containing E3 ubiquitin protein ligase 1 (*WWP1*), Runx2, and JunB (**d**) in MC3T3-E1 cells. The cells were harvested after treatment with 200 μM agomir, antagomir, or the corresponding controls for 48 h. All data are the mean ± standard deviation from five independent experiments. *AgomiR-NC*, negative control agomir, *antagomiR-NC*, negative control antagomir, *CDS* coding DNA sequence, *Mut*, *MUT* mutant, *WT* wild type, *asterisk P* < 0.05

and mineralization by osteoblasts [33–35]. In this study, we clarified that miR-142-5p promoted bone repair by stimulating osteoblast activity. Moreover, miR-142-5p expression significantly decreased in aged mice with delayed fracture healing, and treatment with agomir-142-5p at fracture sites promoted bone formation and bone healing. Hence, this study identified miR-142-5p as an important stimulator of osteoblast activity and bone repair under both physiological and pathophysiological conditions.

Multiple miRNAs act as important regulators of osteoblast-related gene expression at the posttranscriptional level [36–40]. They might regulate gene expression either by increasing mRNA decomposition or by repressing protein translation. There are many examples that miRNAs downregulate protein accumulation without influencing the levels of mRNA [41, 42], suggesting that translation is inhibited after its initiation [43]. This provides an explanation for unchanged *Wwp1* mRNA and upregulated WWP1

protein levels in our study, indicating that miR-142-5p affects WWP1 translation rather than mRNA itself.

So far, the existing evidence has confirmed the essential roles of miRNAs in bone development and homeostasis. Deregulation of miRNA-mediated mechanisms is emerging as a vital pathological factor in skeletal disorders. However, few reports are available concerning miRNAs that modulate fracture healing or therapeutic approaches using miRNAs to promote fracture healing.

In our study, we found a dramatic activation of miR-142-5p expression in osteoblasts, whereas downregulation of miR-142-5p expression reduced the mRNA levels of Runx2, JunB, and osteocalcin, suggesting miR-142-5p enhanced osteoblast activity and matrix mineralization during the bone healing process. The pattern of miR-142-5p expression was positively correlated with the expression of bone formation marker genes. Thus, our study revealed that miR-142-5p promotes fracture healing via activation of
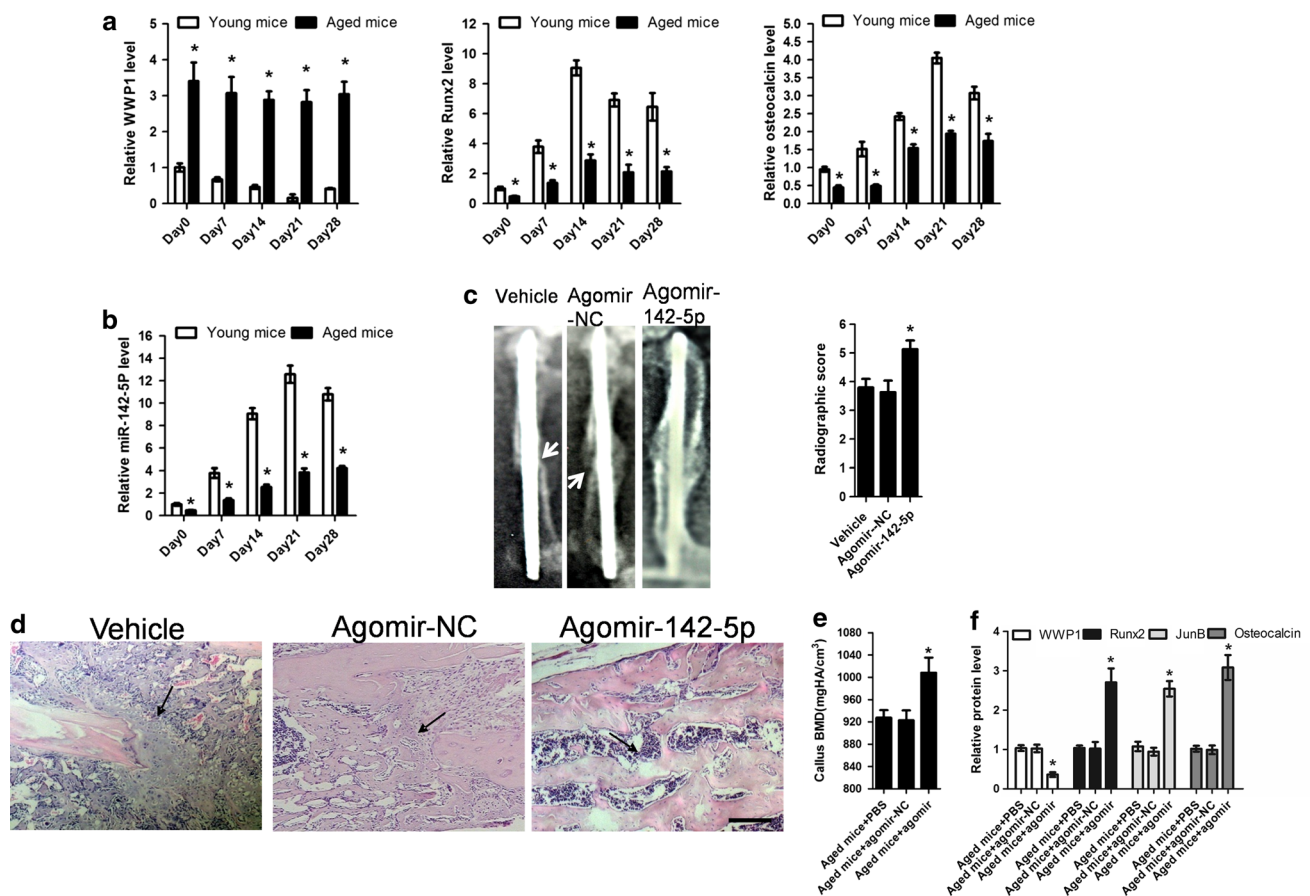
Fig. 4 Age-related bone healing delay was associated with bone callus miR-142-5p. **a** Total RNA was harvested from fracture callus in young and aged mice on days 7, 14, 21, and 28 after fracture. WW-domain-containing E3 ubiquitin protein ligase 1 (*WWP1*), Runx2, and osteocalcin levels were determined by Western blot, and the acquired band intensities were normalized to the ratio of the internal standard β-actin and expressed as a value relative to the mean intensity at the intact femur (nonfractured; day 0) from young mice. **b** The miR-142-5p level was determined by quantitative reverse transcription PCR in callus at different time points (days 0, 7, 14, 21, and 28 after fracture) from young and aged mice with stabilized femoral fractures, and the acquired band intensities were normalized to the ratio of the internal standard U6 and expressed as a value relative to the mean intensity at the intact femur (nonfractured; day 0). **c** Representative radiographs and radiographic scores of vehicle-treated aged mice, negative control agomir (*agomir-NC*)-treated aged mice, and agomir-142-5p-treated aged mice at 28 days after fracture. **d** Representative hematoxylin–eosin-stained sections of vehicle-treated aged mice, agomir-NC-treated aged mice, and agomir-142-5p-treated aged mice at 28 days after fracture shown (*scale bar* 100 µm). **e** Three-dimensional micro-CT quantification of volumetric density (mg hydroxyapatite/cm³) of the mineralized tissue (*BMD*), expressed as a fraction of mineralized tissue within the callus, excluding the original tibia shaft in aged mice into which agomir-142-5p (*aged mice+agomir*), agomir-NC (*aged mice+agomir-NC*) or phosphate-buffered saline (PBS; *aged mice+PBS*) was injected at day 28 after fracture. **f** Western blot analysis of WWP1, Runx2, JunB, and osteocalcin in the callus at day 28 from aged mice into which agomir-142-5p (*aged mice+agomir*), agomir-NC (*aged mice+agomir-NC*), or PBS (*aged mice+PBS*) was injected. The acquired band intensities were normalized to the ratio of the internal standard β-actin and expressed as a value relative to the mean intensity at the callus (day 28) from the PBS group (aged mice+PBS). All data are the mean ± standard deviation from five independent experiments. *Asterisk* $P < 0.05$

osteoblast activity, and is an important regulator of osteoblast function. To our knowledge, these results are the first to demonstrate the role of miR-142-5p in fracture healing. Our data highlight the role of miRNAs in osteogenesis and emphasize their potential therapeutic values for bone abnormalities.

WWP1 belongs to the C2-WW-HECT subfamily of ubiquitin E3 ligases [32]. Previous studies have reported that TNF-induced effects on mesenchymal colony formation, osteoblast differentiation, and JunB ubiquitination were abolished in $Wwp1^{-/-}$ mice [44]. These studies demonstrated that $Wwp1^{-/-}$ mice developed increased bone mass as they aged, associated with increased bone formation rates and normal bone resorption parameters. They indicated WWP1 is a negative regulator of osteoblast differentiation. Our data demonstrated that the change in miR-142-5p level results in an alteration in the expression of WWP1. MiR-142-5p stimulates osteocalcin and Runx2

expression by targeting *Wwp1*. Furthermore, our experimental evidence strongly suggests that *Wwp1* is a functional target of miR-142-5p, mediating the regulation of the effect of miR-142-5p on osteoblast function. This is the first report identifying *Wwp1* as a negative target of miR-142-5p during the fracture healing process. We plan to test the effect of miR-142-5p in *Wwp1*-deficient conditions. Additionally, we will test the involvement of other target genes in the miR-142-5p-mediated bone healing process.

The capacity for bone repair declines with age. Previous studies of fracture healing in rats have shown that osteoblast activity, bone formation, and accretion of mineral into the callus decreased in elderly animals. In this study, we found that miR-142-5p concentrations in the callus of aged mice were lower than those in the callus of young mice and directly correlated with the age-related delay in bone healing. Notably, local upregulation of miR-142-5p expression caused by agomir-142-5p restored the impaired osteoblast activity and fracture repair in aged mice. These data suggest that the lower miR-142-5p levels in the callus contribute to the delayed fracture healing in aged mice. Agomir-142-5p treatment could potentially be a promising way of experimentation to develop novel therapies for treating patients with delayed fracture healing.

Thus, our study provides a new finding that the activation of miR-142-5p during bone fracture promotes osteoblast activity in vitro and in vivo, and this specific miRNA could be targeted to improve fracture healing in the aging process.

Compliance with ethical standards

Conflict of interest The authors declare that they have no conflict of interest.

References

1. Gardner MJ, Demetrakopoulos D, Shindle MK, Griffith MH, Lane JM (2006) Osteoporosis and skeletal fractures. HSS J 2:62–69
2. Chrischilles EA, Butler CD, Davis CS, Wallace RB (1991) A model of lifetime osteoporosis impact. Arch Intern Med 151:2026–2032
3. Riggs BL, Melton LJ 3rd (1995) The worldwide problem of osteoporosis: insights afforded by epidemiology. Bone 17:505S–511S
4. Nelson FR, Brighton CT, Ryaby J, Simon BJ, Nielson JH, Lorich DG, Bolander M, Seelig J (2003) Use of physical forces in bone healing. J Am Acad Orthop Surg 11:344–354
5. Rozen N, Lewinson D, Bick T, Meretyk S, Soudry M (2007) Role of bone regeneration and turnover modulators in control of fracture. Crit Rev Eukaryot Gene Expr 17:197–213
6. Mehta M, Strube P, Peters A, Perka C, Hutmacher D, Fratzl P, Duda GN (2010) Influences of age and mechanical stability on volume, microstructure, and mineralization of the fracture callus during bone healing: is osteoclast activity the key to age-related impaired healing? Bone 47:219–228
7. Claes L, Recknagel S, Ignatius A (2012) Fracture healing under healthy and inflammatory conditions. Nat Rev Rheumatol 8:133–143
8. Ai-Aql ZS, Alagl AS, Graves DT, Gerstenfeld LC, Einhorn TA (2008) Molecular mechanisms controlling bone formation during fracture healing and distraction osteogenesis. J Dent Res 87:107–118
9. Nilsson BE, Edwards P (1969) Age and fracture healing: a statistical analysis of 418 cases of tibial shaft fractures. Geriatrics 24:112–117
10. Ekeland A, Engesoeter LB, Langeland N (1982) Influence of age on mechanical properties of healing fractures and intact bones in rats. Acta Orthop Scand 53:527–534
11. Meyer RA Jr, Tsahakis PJ, Martin DF, Banks DM, Harrow ME, Kiebzak GM (2001) Age and ovariectomy impair both the normalization of mechanical properties and the accretion of mineral by the fracture callus in rats. J Orthop Res 19:428–435
12. Naik AA, Xie C, Zuscik MJ, Kingsley P, Schwarz EM, Awad H, Guldberg R, Drissi H, Puzas JE, Boyce B et al (2009) Reduced COX-2 expression in aged mice is associated with impaired fracture healing. J Bone Miner Res 24:251–264
13. Meyer RA, Meyer MH, Phieffer LS, Banks DM (2001) Delayed union of femoral fractures in older rats: decreased gene expression. BMC Musculoskelet Disord 2:2
14. Carthew RW, Sontheimer EJ (2009) Origins and mechanisms of miRNAs and siRNAs. Cell 136:642–655
15. Inose H, Ochi H, Kimura A, Fujita K, Xu R, Sato S, Iwasaki M, Sunamura S, Takeuchi Y, Fukumoto S et al (2009) A microRNA regulatory mechanism of osteoblast differentiation. Proc Natl Acad Sci U S A 106:20794–20799
16. Li Z, Hassan MQ, Volinia S, van Wijnen AJ, Stein JL, Croce CM, Lian JB, Stein GS (2008) A microRNA signature for a BMP2-induced osteoblast lineage commitment program. Proc Natl Acad Sci U S A 105:13906–13911
17. Kobayashi T, Lu J, Cobb BS, Rodda SJ, McMahon AP, Schipani E, Merkenschlager M, Kronenberg HM (2008) Dicer-dependent pathways regulate chondrocyte proliferation and differentiation. Proc Natl Acad Sci U S A 105:1949–1954
18. Wei J, Shi Y, Zheng L, Zhou B, Inose H, Wang J, Guo XE, Grosschedl R, Karsenty G (2012) miR-34s inhibit osteoblast proliferation and differentiation in the mouse by targeting SATB2. J Cell Biol 197:509–521
19. Hu R, Liu W, Li H, Yang L, Chen C, Xia ZY, Guo LJ, Xie H, Zhou HD, Wu XP et al (2011) A Runx2/miR-3960/miR-2861 regulatory feedback loop during mouse osteoblast differentiation. J Biol Chem 286:12328–12339
20. Li H, Xie H, Liu W, Hu R, Huang B, Tan YF, Xu K, Sheng ZF, Zhou HD, Wu XP et al (2009) A novel microRNA targeting HDAC5 regulates osteoblast differentiation in mice and contributes to primary osteoporosis in humans. J Clin Invest 119:3666–3677
21. Wang X, Guo B, Li Q, Peng J, Yang Z, Wang A, Li D, Hou Z, Lv K, Kan G et al (2013) miR-214 targets ATF4 to inhibit bone formation. Nat Med 19:93–100
22. Murata K, Ito H, Yoshitomi H, Yamamoto K, Fukuda A, Yoshikawa J, Furu M, Ishikawa M, Shibuya H, Matsuda S (2014) Inhibition of miR-92a enhances fracture healing via promoting

angiogenesis in a model of stabilized fracture in young mice. J Bone Miner Res 29:316–326

23. Zhang X, Yan Z, Zhang J, Gong L, Li W, Cui J, Liu Y, Gao Z, Li J, Shen L et al (2011) Combination of hsa-miR-375 and hsa-miR-142-5p as a predictor for recurrence risk in gastric cancer patients following surgical resection. Ann Oncol 22:2257–2266

24. Schaefer JS, Montufar-Solis D, Vigneswaran N, Klein JR (2011) Selective upregulation of microRNA expression in peripheral blood leukocytes in IL-10$^{-/-}$ mice precedes expression in the colon. J Immunol 187:5834–5841

25. Chaudhuri AD, Yelamanchili SV, Marcondes MC, Fox HS (2013) Up-regulation of microRNA-142 in simian immunodeficiency virus encephalitis leads to repression of sirtuin1. FASEB J 27:3720–3729

26. Xu R, Bi C, Song J, Wang L, Ge C, Liu X, Zhang M (2015) Upregulation of miR-142-5p in atherosclerotic plaques and regulation of oxidized low-density lipoprotein-induced apoptosis in macrophages. Mol Med Rep 11:3229–3234

27. Jones KB, Salah Z, Del Mare S, Galasso M, Gaudio E, Nuovo GJ, Lovat F, LeBlanc K, Palatini J, Randall RL et al (2012) miRNA signatures associate with pathogenesis and progression of osteosarcoma. Cancer Res 72:1865–1877

28. Zhao R, Zhu Y, Sun B (2015) Exploration of the effect of mmu-miR-142-5p on osteoblast and the mechanism. Cell Biochem Biophys 71:255–260

29. Manigrasso MB, O'Connor JP (2004) Characterization of a closed femur fracture model in mice. J Orthop Trauma 18:687–695

30. Cho TJ, Gerstenfeld LC, Einhorn TA (2002) Differential temporal expression of members of the transforming growth factor beta superfamily during murine fracture healing. J Bone Miner Res 17:513–520

31. Garcia DM, Baek D, Shin C, Bell GW, Grimson A, Bartel DP (2011) Weak seed-pairing stability and high target-site abundance decrease the proficiency of lsy-6 and other microRNAs. Nat Struct Mol Biol 18:1139–1146

32. Shu L, Zhang H, Boyce BF, Xing L (2013) Ubiquitin E3 ligase Wwp1 negatively regulates osteoblast function by inhibiting osteoblast differentiation and migration. J Bone Miner Res 28:1925–1935

33. Phillips AM (2005) Overview of the fracture healing cascade. Injury 36:S5–S7

34. Ferguson CM, Miclau T, Hu D, Alpern E, Helms JA (1998) Common molecular pathways in skeletal morphogenesis and repair. Ann N Y Acad Sci 857:33–42

35. Einhorn TA (1998) The cell and molecular biology of fracture healing. Clin Orthop Relat Res (355 Suppl):S7–S21

36. Hassan MQ, Gordon JA, Beloti MM, Croce CM, van Wijnen AJ, Stein JL, Stein GS, Lian JB (2010) A network connecting Runx2, SATB2, and the miR-23a–27a–24-2 cluster regulates the osteoblast differentiation program. Proc Natl Acad Sci U S A 107:19879–19884

37. Li Z, Hassan MQ, Jafferji M, Aqeilan RI, Garzon R, Croce CM, van Wijnen AJ, Stein JL, Stein GS, Lian JB (2009) Biological functions of miR-29b contribute to positive regulation of osteoblast differentiation. J Biol Chem 284:15676–15684

38. Zhang Y, Xie RL, Croce CM, Stein JL, Lian JB, van Wijnen AJ, Stein GS (2011) A program of microRNAs controls osteogenic lineage progression by targeting transcription factor Runx2. Proc Natl Acad Sci U S A 108:9863–9868

39. Yang L, Cheng P, Chen C, He HB, Xie GQ, Zhou HD, Xie H, Wu XP, Luo XH (2012) miR-93/Sp7 function loop mediates osteoblast mineralization. J Bone Miner Res 27:1598–1606

40. Vimalraj S, Selvamurugan N (2013) MicroRNAs: synthesis, gene regulation and osteoblast differentiation. Curr Issues Mol Biol 15:7–18

41. Brennecke J, Hipfner DR, Stark A, Russell RB, Cohen SM (2003) bantam encodes a developmentally regulated microRNA that controls cell proliferation and regulates the proapoptotic gene hid in Drosophila. Cell 113:25–36

42. Chen X (2004) A microRNA as a translational repressor of APETALA2 in Arabidopsis flower development. Science 303:2022–2025

43. Olsen PH, Ambros V (1999) The lin-4 regulatory RNA controls developmental timing in *Caenorhabditis elegans* by blocking LIN-14 protein synthesis after the initiation of translation. Dev Biol 216:671–680

44. Zhao L, Huang J, Zhang H, Wang Y, Matesic LE, Takahata M, Awad H, Chen D, Xing L (2011) Tumor necrosis factor inhibits mesenchymal stem cell differentiation into osteoblasts via the ubiquitin E3 ligase Wwp1. Stem Cells 29:1601–1610